Biomedical Optics EXPRESS

Temporal correlation of spontaneous hemodynamic activity in language areas measured with functional near-infrared spectroscopy

Jun Li* **and Lina Qiu**

South China Academy of Advanced Optoelectronics, South China Normal University, Guangzhou, 510006, China
*jun.li@coer-scnu.org

Abstract: Functional near-infrared spectroscopy (fNIRS) was used to investigate resting state connectivity of language areas including bilateral inferior frontal gyrus (IFG) and superior temporal gyrus (STG). Thirty-two subjects participated in the experiment, including twenty adults and twelve children. Spontaneous hemodynamic fluctuations were recorded, and then intra- and inter-hemispheric temporal correlations of these signals were computed. The correlations of all hemoglobin components were observed significantly higher for adults than children. Moreover, the differences for the STG were more significant than for the IFG. In the adult group, differences in the correlations between males and females were not significant. Our results suggest by measuring resting state intra- and inter-hemispheric correlations, fNIRS is able to provide qualitative and quantitative evaluation on the functioning of the cortical network.

OCIS codes: (170.2655) Functional monitoring and imaging; (170.3880) Medical and biological imaging; (170.5380) Physiology.

References and links

1. F. F. Jöbsis, "Noninvasive, infrared monitoring of cerebral and myocardial oxygen sufficiency and circulatory parameters," Science **198**(4323), 1264–1267 (1977).
2. A. Villringer and B. Chance, "Non-invasive optical spectroscopy and imaging of human brain function," Trends Neurosci. **20**(10), 435–442 (1997).
3. G. Gratton and M. Fabiani, "Dynamic brain imaging: Event-related optical signal (EROS) measures of the time course and localization of cognitive-related activity," Psychon. Bull. Rev. **5**(4), 535–563 (1998).
4. M. Wolf, U. Wolf, J. H. Choi, R. Gupta, L. P. Safonova, L. A. Paunescu, A. Michalos, and E. Gratton, "Functional frequency-domain near-infrared spectroscopy detects fast neuronal signal in the motor cortex," Neuroimage **17**(4), 1868–1875 (2002).
5. Y. Hoshi, "Functional near-infrared optical imaging: Utility and limitations in human brain mapping," Psychophysiology **40**(4), 511–520 (2003).
6. E. M. C. Hillman, "Optical brain imaging in vivo: techniques and applications from animal to man," J. Biomed. Opt. **12**(5), 051402 (2007).
7. M. Wolf, M. Ferrari, and V. Quaresima, "Progress of near-infrared spectroscopy and topography for brain and muscle clinical applications," J. Biomed. Opt. **12**(6), 062104 (2007).
8. T. Funane, M. Kiguchi, H. Atsumori, H. Sato, K. Kubota, and H. Koizumi, "Synchronous activity of two people's prefrontal cortices during a cooperative task measured by simultaneous near-infrared spectroscopy," J. Biomed. Opt. **16**(7), 077011 (2011).
9. V. Quaresima, S. Bisconti, and M. Ferrari, "A brief review on the use of functional near-infrared spectroscopy (fNIRS) for language imaging studies in human newborns and adults," Brain Lang. **121**(2), 79–89 (2012).
10. P. Y. Lin, S. I. Lin, T. Penney, and J. J. Chen, "Applications of Near Infrared Spectroscopy and Imaging for Motor Rehabilitation in Stroke Patients," J. Med. Biol. Eng. **29**, 210–221 (2009).
11. B. Biswal, F. Z. Yetkin, V. M. Haughton, and J. S. Hyde, "Functional connectivity in the motor cortex of resting human brain using echo-planar MRI," Magn. Reson. Med. **34**(4), 537–541 (1995).
12. M. D. Greicius, B. Krasnow, A. L. Reiss, and V. Menon, "Functional connectivity in the resting brain: A network analysis of the default mode hypothesis," Proc. Natl. Acad. Sci. U.S.A. **100**(1), 253–258 (2003).

#200752 - $15.00 USD Received 5 Nov 2013; revised 19 Jan 2014; accepted 20 Jan 2014; published 24 Jan 2014

13. H. D. Xiang, H. M. Fonteijn, D. G. Norris, and P. Hagoort, "Topographical functional connectivity pattern in the perisylvian language networks," Cereb. Cortex **20**(3), 549–560 (2010).
14. D. A. Fair, A. L. Cohen, N. U. Dosenbach, J. A. Church, F. M. Miezin, D. M. Barch, M. E. Raichle, S. E. Petersen, and B. L. Schlaggar, "The maturing architecture of the brain's default network," Proc. Natl. Acad. Sci. U.S.A. **105**(10), 4028–4032 (2008).
15. B. R. White, A. Z. Snyder, A. L. Cohen, S. E. Petersen, M. E. Raichle, B. L. Schlaggar, and J. P. Culver, "Resting-state functional connectivity in the human brain revealed with diffuse optical tomography," Neuroimage **47**(1), 148–156 (2009).
16. C. M. Lu, Y. J. Zhang, B. B. Biswal, Y. F. Zang, D. L. Peng, and C. Z. Zhu, "Use of fNIRS to assess resting state functional connectivity," J. Neurosci. Methods **186**(2), 242–249 (2010).
17. R. C. Mesquita, M. A. Franceschini, and D. A. Boas, "Resting state functional connectivity of the whole head with near-infrared spectroscopy," Biomed. Opt. Express **1**(1), 324–336 (2010).
18. H. Zhang, L. Duan, Y. J. Zhang, C. M. Lu, H. Liu, and C. Z. Zhu, "Test-retest assessment of independent component analysis-derived resting-state functional connectivity based on functional near-infrared spectroscopy," Neuroimage **55**(2), 607–615 (2011).
19. L. Duan, Y. J. Zhang, and C. Z. Zhu, "Quantitative comparison of resting-state functional connectivity derived from fNIRS and fMRI: A simultaneous recording study," Neuroimage **60**(4), 2008–2018 (2012).
20. F. Homae, H. Watanabe, T. Otobe, T. Nakano, T. Go, Y. Konishi, and G. Taga, "Development of global cortical networks in early infancy," J. Neurosci. **30**(14), 4877–4882 (2010).
21. P. Hagmann, L. Cammoun, R. Martuzzi, P. Maeder, S. Clarke, J. P. Thiran, and R. Meuli, "Hand Preference and Sex Shape the Architecture of Language Networks," Hum. Brain Mapp. **27**(10), 828–835 (2006).
22. N. F. Dronkers, D. P. Wilkins, R. D. Van Valin, Jr., B. B. Redfern, and J. J. Jaeger, "Lesion analysis of the brain areas involved in language comprehension," Cognition **92**(1-2), 145–177 (2004).
23. M. A. Gernsbacher and M. P. Kaschak, "Neuroimaging Studies of Language Production and Comprehension," Annu. Rev. Psychol. **54**(1), 91–114 (2003).
24. R. C. Martin, "Language Processing: Functional Organization and Neuroanatomical Basis," Annu. Rev. Psychol. **54**(1), 55–89 (2003).
25. I. Dinstein, K. Pierce, L. Eyler, S. Solso, R. Malach, M. Behrmann, and E. Courchesne, "Disrupted neural synchronization in toddlers with autism," Neuron **70**(6), 1218–1225 (2011).
26. I. E. C. Sommer, A. Aleman, A. Bouma, and R. S. Kahn, "Do women really have more bilateral language representation than men? A meta-analysis of functional imaging studies," Brain **127**(8), 1845–1852 (2004).
27. M. Wallentin, "Putative sex differences in verbal abilities and language cortex: a critical review," Brain Lang. **108**(3), 175–183 (2009).
28. A. Hyvärinen and E. Oja, "Independent Component Analysis: Algorithms and Applications," Neural Netw. **13**(4-5), 411–430 (2000).
29. J. A. Frost, J. R. Binder, J. A. Springer, T. A. Hammeke, P. S. F. Bellgowan, S. M. Rao, and R. W. Cox, "Language processing is strongly left lateralized in both sexes. Evidence from functional MRI," Brain **122**(2), 199–208 (1999).
30. K. Murphy, R. M. Birn, D. A. Handwerker, T. B. Jones, and P. A. Bandettini, "The impact of global signal regression on resting state correlations: are anti-correlated networks introduced?" Neuroimage **44**(3), 893–905 (2009).
31. L. Gagnon, K. Perdue, D. N. Greve, D. Goldenholz, G. Kaskhedikar, and D. A. Boas, "Improved recovery of the hemodynamic response in diffuse optical imaging using short optode separations and state-space modeling," Neuroimage **56**(3), 1362–1371 (2011).
32. L. Gagnon, R. J. Cooper, M. A. Yücel, K. L. Perdue, D. N. Greve, and D. A. Boas, "Short separation channel location impacts the performance of short channel regression in NIRS," Neuroimage **59**(3), 2518–2528 (2012).
33. L. Gagnon, M. A. Yücel, D. A. Boas, and R. J. Cooper, "Further improvement in reducing superficial contamination in NIRS using double short separation measurements," Neuroimage **85**(Pt 1), 127–135 (2014).
34. A. D. Friederici, J. Brauer, and G. Lohmann, "Maturation of the language network: from inter- to intrahemispheric connectivities," PLoS ONE **6**(6), e20726 (2011).

1. Introduction

Functional near-infrared spectroscopy (fNIRS) is a non-invasive optical technique that can be used for investigating brain functional activity [1–10]. Since the seminal work of Jöbsis demonstrating the possibility of using near-infrared light to non-invasively probe cortical functioning [1], various techniques have been developed for imaging the brain, including continuous-wave, time-resolved and frequency-domain modalities [5–7].

fNIRS detects concentration changes in cortical hemoglobin associated with neural activity through the neurovascular coupling. Thus the physiological basis of fNIRS is similar to functional magnetic resonance imaging (fMRI). Due to the limited penetration depth of near infrared light in tissues, fNIRS provides a 2-demensional functional map with sub-

#200752 - $15.00 USD Received 5 Nov 2013; revised 19 Jan 2014; accepted 20 Jan 2014; published 24 Jan 2014

centimeter spatial resolution, containing hemodynamic information in the cortex about 2 cm below the scalp.

Despite the limited probing depth and rough spatial resolution, fNIRS has been widely used in a variety of areas ranging from basic neuroscience research to psychological and clinical applications [3,4, 8–10], because most of the functional cortex is located just below the skull where fNIRS is able to interrogate. Although sub-centimeter spatial resolution is far from fine for imaging, it is still acceptable for studying functional areas, including frontal [5, 8], parietal [4], temporal [9] and occipital cortices [3].

For years, fNIRS has been used to study task-related cortical activities, including but not limited to motor cortex activation induced by finger-tapping tasks [4], visual cortical activity elicited by visual stimuli [3], enhanced left frontal cortical activity in a N-back memory task [5]. These studies are in agreement with previous observations obtained with other brain imaging modalities, demonstrating the ability of fNIRS for probing functioning brain.

Resting state functional connectivity was previously identified in fMRI, where the low frequency (<0.1 Hz) spontaneous blood oxygen level dependent (BOLD) fluctuations were observed to be temporally correlated in functionally connected cortical regions, even across the two hemispheres [11–14]. It reveals the fact that the spontaneous brain activities in these regions (neighboring and/or remote) are synchronized.

Very recently, the resting state brain has also been studied by fNIRS, where the spontaneous cerebral hemodynamic fluctuations are measured [15–20]. These studies show in healthy subjects there exist robust intra- and/or inter-hemispheric correlations across functional regions, such as prefrontal, sensorimotor, and visual cortices [17]. These correlations reveal brain functional architecture, connectivity (or neural networks), and synchronization of brain activities.

In this work, resting state hemodynamic fluctuations were measured with fNIRS in the left and right cortical language areas for adults and children. The IFG is responsible for language production, whereas the STG contributes to language comprehension [21–24]. The language areas were selected for this study because their locations are relatively close to the scalp surface; therefore it is possible for fNIRS to sample these regions. On the other hand, the language areas are of great interest to neuroscientists and clinicians, because its functional state is linked to neural diseases and developmental problems, such as autism and speech problems [25].

Temporal intra-hemispheric and inter-hemispheric correlations for the language regions were calculated for each subject. Our hypothesis was language ability for adults is better than children, which might be reflected by the differences in the intra-hemispheric and/or inter-hemispheric correlations between adults and children. In the adult group, differences in the correlation between males and females were also compared, since there has been a debate in the literature on whether there are sex differences in language cortex [26,27]. To our best knowledge, this is the first study to use fNIRS to reveal developmental and sex differences in the cortical connectivity in the language areas.

2. Methods

2.1 Experimental setup

Measurements were performed with a commercial continuous-wave fNIRS system (FOIRE-3000, Shimadzu Corporation, Kyoto, Japan) working at three different wavelengths, 780 nm, 805 nm and 830 nm. FOIRE-3000 is equipped with sixteen fiber sources and sixteen fiber detectors, building up to fifty two detecting channels with a fixed source-detector distance of 3.0 cm. Parameters measured are concentration changes in oxygenated hemoglobin (HBO), deoxygenated hemoglobin (HB) and total hemoglobin (HBT) based on the modified Beer-Lambert law.

#200752 - $15.00 USD Received 5 Nov 2013; revised 19 Jan 2014; accepted 20 Jan 2014; published 24 Jan 2014

2.2 Subjects and experimental protocol

Thirty-two healthy right-handed subjects (twenty adults and twelve children) participated in this study. In the adult group, there were ten subjects for each sex, all recruited from the university student body. The average age was 23.4 (± 0.9) years old (male: 22-25 years old, female: 22-24 years old). The children group consisted of eight boys and four girls with the average age of 9.0 (± 1.5) years old.

During the experiment, subjects were sitting in a comfortable chair in a dark room, and asked to close their eyes and keep quiet. The optical sensors were secured on the scalp by a headgear to ensure good sensor-scalp contact. To identify locations of IFG and STG, the international 10-20 system for electroencephalography (EEG) was referenced with a EEG cap, in which F7 (F8) and CP5 (CP6) correspond to IFG and STG. Forty four channels (twenty two for each hemisphere, covering IFG, STG and their surrounding areas) were used for recording 8 minutes of spontaneous cerebral homodynamic fluctuations with a 70 ms temporal resolution. Our source-detector grid and channel locations over language areas are schematically shown in Fig. 1. Prior to the experiment, subjects were informed about the measuring procedure and written consent was obtained from the adult group and the parents of the children group. The study protocol was approved by the University's Ethical Review Board.

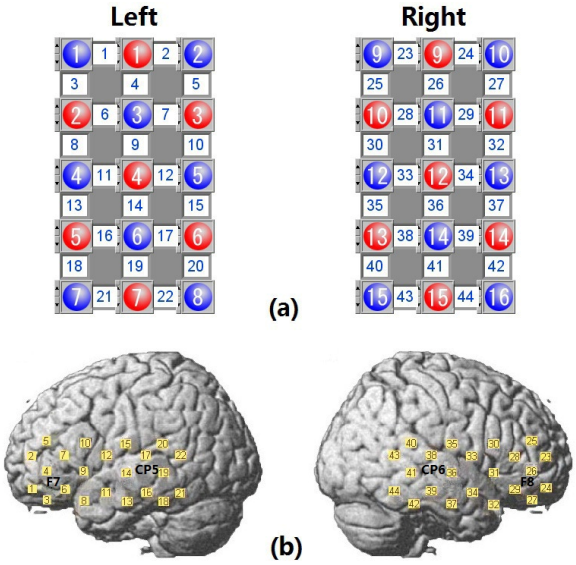

Fig. 1. Experimental schematics- (a) The schematic of source-detector grid where the red circles represent the sources, and the blue circles represent the detectors, and the square between a source and a detector is a channel. (b). Schematic (or visual) representation of the brain showing the location of each measurement channel. The 10-20 EEG sites F7, CP5, F8, and CP6 are also marked.

2.3 Data analysis

The raw temporal hemodynamic data (HBO, HB and HBT) was fitted using a second order polynomial fit to remove the first- and second-order drift [19], and then a low frequency band-pass filter (0.009-0.08 Hz) was applied [15,17].

After the band-pass filter, most systemic hemodynamic components were filtered out, such as those originated from heartbeats (~1 Hz), venous pressure waves due to respiration (~0.2 Hz) and arterial pressure oscillations (Mayer waves ~0.1 Hz). However, the measured

#200752 - $15.00 USD Received 5 Nov 2013; revised 19 Jan 2014; accepted 20 Jan 2014; published 24 Jan 2014

signal at each channel might be still mixed with a low frequency global component that was not specific to local cortex. To remove this remaining global component, an independent component analysis (ICA) algorithm [28] was used, which will be discussed in detail in the Discussion section.

The temporal correlation between each channel pair was presented as Pearson correlation coefficient. In order to obtain an average correlation coefficient for all channel pairs in an area of interest, the Fisher Z transform function was applied to each individual correlation coefficient to get a z value. After averaging the z values, the inverse Fisher transform was used, which gave the average value of the correlation coefficients.

A correlation map visually shows the correlation (or synchronization) pattern of cortical spontaneous activity in a mapping area. To make a correlation map, first, a seed channel is selected, and then the temporal correlation coefficients between the seed channel and the all other channels in the areas of interest are calculated. Finally a false color map is made where the color value for each pixel represents the correlation coefficient between this pixel (channel) and the seed pixel (channel).

One data set from the children group was discarded in data analysis due to large motion-induced artifacts.

3. Results

Figure 2 shows the average HBO correlation maps of adults [N = 20, Figs. 2(a) and 2(b)] and children [N = 11, Figs. 2(c) and 2(d)] for the IFG, and the STG areas. The left (right) IFG map includes channel-1 to channel-10 (channel-23 to channel-32), while the left (right) STG map includes channel-11 to channel-22 (channel-33 to channel-44). Since language production and comprehension rely mainly on left hemispheric networks [29], the seeds for generating correlation maps were selected on the left hemisphere, around F7 and CP5 for the IFG and STG maps, respectively.

For the adult group, strong local intra-hemispherical correlation around the seeds on the left hemisphere can be clearly seen on both the IFG and the STG maps. The STG map shows stronger inter-hemispheric correlation than the IFG map. Symmetric patterning across the two hemispheres can be seen in the STG map, while in the IFG map, the symmetry is not pronounced.

Similar to the pattern of the adult group, the local intra-hemispheric correlation for the children group can be observed in the left IFG and STG maps. However, the children group differs from the adult group in two significant ways, namely, the correlation range or the spatial extent of local correlation around the seed in the IFG and the STG maps is smaller and the inter-hemispheric correlations are smaller.

The HB and HBT correlation maps are not presented, as they are similar to the HBO.

To quantitatively compare the inter-hemispheric correlations between adults and children, the average correlation coefficients between the left and right corresponding channel pairs were calculated for the two groups, and illustrated in Fig. 3.

For all three hemoglobin components, the average inter-hemispheric correlation coefficients are larger for the adult group than for the children group in all areas of interest (IFG, STG and the Whole = IFG + STG). To verify the significance of the differences between the two groups, the two-sample t-test was performed, which gave p-values of: p (Whole) = 0.0024, p (IFG) = 0.0207 and p (STG) = 0.0002 for HBO; p (Whole) = 0.0245, p (IFG) = 0.0671 and p (STG) = 0.0090 for HB; p (Whole) = 3.2×10^{-7}, p (IFG) = 2.0×10^{-4} and p (STG) = 7.1×10^{-10} for HBT. All p-values, except p (IFG) for HB, are smaller than 0.05, demonstrating that the inter-hemispheric correlation differences are significant between the adult and the children group. Moreover, the differences in STG are more pronounced. These findings are in line with the fact that language ability is better for adults than for children whose cortices are still developing.

#200752 - $15.00 USD Received 5 Nov 2013; revised 19 Jan 2014; accepted 20 Jan 2014; published 24 Jan 2014

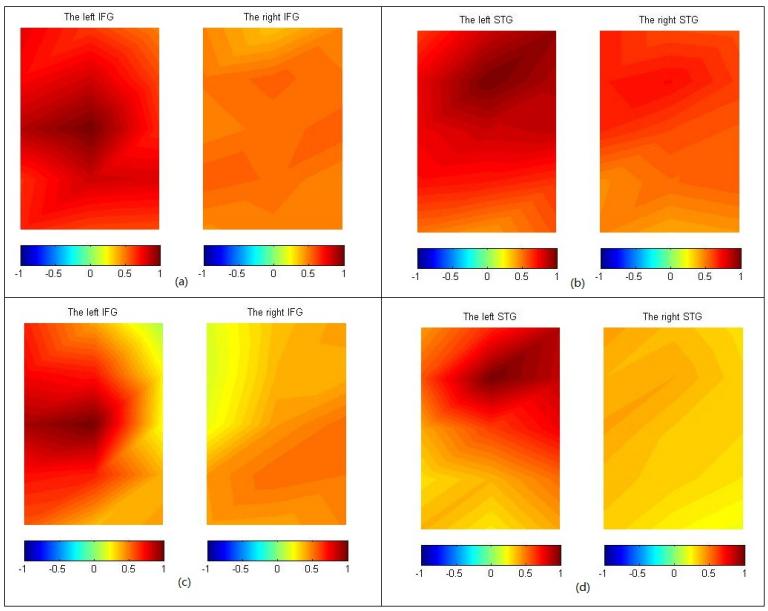

Fig. 2. HBO correlation maps of the adults [(a) and (b)] and children [(c) and (d)] for IFG and STG. The seeds are located on the left hemisphere and can be visually recognized by the maximal color value in each map.

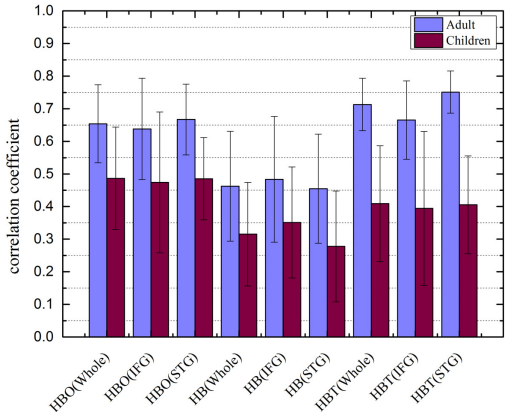

Fig. 3. Comparison between the adult and children group in the average correlation coefficients of HBO, HB and HBT across two hemispheres in 3 areas of interest: IFG, STG and the whole (IFG + STG). The average and standard deviation were calculated for each group. Differences between adults and children are statistically significant for all cases, except for HB (IFG).

Figure 4 shows the inter-hemispheric correlation coefficients for the bilateral language areas averaged across the adult male and female groups. The average values for females are larger than males in all areas of interest. However, the two-sample t-test shows these differences are not significant ($p>0.05$), except for HBT in STG ($p = 0.0485$) is marginally significant. Therefore the bilateral network connectivity for language areas is not significantly differentiable between males and females. This may imply that sex differences in language abilities are not pronounced, in agreement with most previous studies with other modalities [26,27].

#200752 - $15.00 USD Received 5 Nov 2013; revised 19 Jan 2014; accepted 20 Jan 2014; published 24 Jan 2014

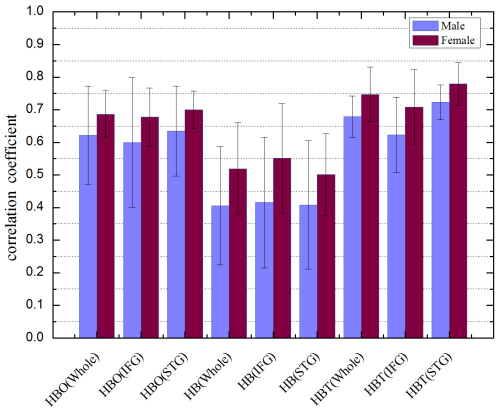

Fig. 4. Comparison between adult male and female subjects in the average correlation coefficients of HBO, HB and HBT across two hemispheres in 3 areas of interest: IFG, STG and the whole (IFG + STG). The average and standard deviation were calculated for each sex. Two-sample t-test shows that only the difference in HBT (STG) is marginally significant ($p = 0.0485<0.05$), while the others are not significant.

4. Discussion

Resting state measurements, in contrast to measurements with tasks, cannot be averaged over block intervals to get rid of noise. Thus the data recorded generally need to be "cleaner" than data in measurement with tasks. During measurements, all subjects were asked to keep quiet and remain motionless as much as possible, which ensured minimal artifacts in the data. Furthermore, before data processing, all temporal data were visually examined to exclude data with large artifacts. In this study, data from one child (7 years old, the youngest recruited in this study) were discarded due to large motion-induced artifacts.

After the low frequency band-pass filter, various global systemic components due to heartbeats, respiration, and Mayer waves, have been filtered out. Still there might be remaining global component mixed in the signals, which results in overestimation of the correlation coefficients. Conventionally, to get rid of the remaining global component, a regression routine is used, in which the global component is assumed to be the overall mean across all measurement channels [30]. This method assumes that local spontaneous fluctuations are uncorrelated each other thus can be averaged out, so that only the global component remains in the overall mean. In fact, this underlying assumption is not true, because the local fluctuations are actually correlated, especially those from neighboring and bilateral corresponding channels. Therefore the global component estimated by this method contains part of local signals, resulting in underestimate on the correlation coefficients, as illustrated in Fig. 5(c).

Instead of using the conventional regression algorithm, an ICA based method [28] was used in this work to eliminate the global components before computing the correlations. The two assumptions made in the ICA method are that the global component is independent with all local signals and that the contribution of the global component to each channel is similar in amplitude. The reason for the second assumption is due to the fact that the same source-detector spacing was used in our measurements. On the other hand, when performing ICA on the experimental data, the mixing matrix always contains a column whose elements have small variation, which means the corresponding ICA component is global and makes similar contributions to each channel. This also supports our assumption.

To verify this ICA method we performed a simulation study in which the simulated pattern was produced from real experimental data [Fig. 5(a)]. In the simulation, an

#200752 - $15.00 USD Received 5 Nov 2013; revised 19 Jan 2014; accepted 20 Jan 2014; published 24 Jan 2014

experimental data matrix (drift-corrected and filtered, rows as variables/channels and columns as observations/time-series) was whitened, so that there was no correlation between each row in the whitened matrix, denoted as **X**. Secondly, one row (can be any row, here the first row in **X**) was selected as a seed, and the other rows were transformed, together with the seed, to build up a new data matrix **Y** with designed correlation coefficients between the first row (the seed) and the other rows. $\mathbf{x}_1$ is the first row in **X** (also in **Y**, namely, $\mathbf{y}_1 = \mathbf{x}_1$), the j-th row $\mathbf{y}_j$ in **Y** will have the correlation coefficient of r with $\mathbf{x}_1$ if, $\mathbf{y}_j = r \cdot \mathbf{x}_1 + \mathbf{x}_j \sqrt{1-r^2}$, $\mathbf{x}_j$ is the j-th row in **X**. A global component with no correlation with any row of **Y** can be added to **Y** to form the final data matrix **Z** for the simulation.

As we assume the global component makes similar contribution to each channel, one independent component is estimated as the global component as long as its corresponding column in the mixing matrix **A** of ICA (**Z** = **A** × **ICAs**) has least variation.

Figure 5 shows the simulation result. Figure 5(a) is the original correlation map generated from matrix **Y** without any global component. After adding a global component to **Y**, the correlation map calculated from **Z** is over-correlated, as is shown in Fig. 5(b), obscuring the original correlation pattern. The conventional regression method excludes not only the global component but also the local signals, resulting in underestimate on the correlations, as can be seen in Fig. 5(c). The ICA method suppresses the global component, and preserves most of the original correlation pattern, as is shown in Fig. 5(d).

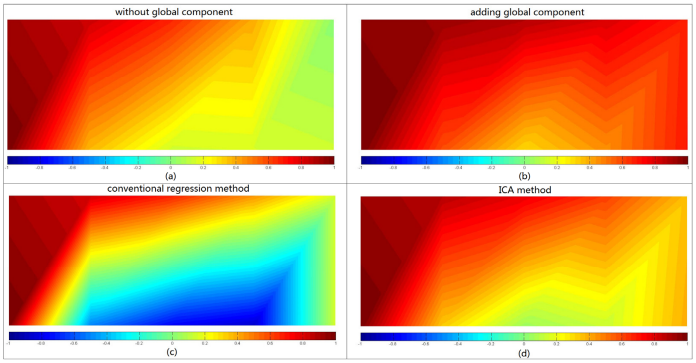

Fig. 5. Simulation study (a) An original correlation map generated from a transform of real experimental data. (b) The addition of a global component to each channel of the original map, results in overestimate in correlations. (c) The conventional regression method to remove the global component underestimates the real correlations seen in (a). (d) Using the ICA method to eliminate the global component faithfully reproduces the qualitative behavior of the correlations seen in (a).

Low frequency hemodynamic fluctuations from the scalp and the skull are probably one of the major sources of the global component of the signals after the band-pass filter. To get rid of the superficial influence, Gagnon et al. [31–33] developed an effective method in which short source-detector spacing probes were used to catch signals only from the scalp and the skull. By using a Kalman filter, the superficial component of the data from large source-detectors was successfully extracted out. Therefore this method can also be used to eliminate the global component originating from the scalp and the skull.

In our study with fNIRS, we observed the local correlation range in the left hemisphere is smaller for children than adults, in both the IFG and STG regions, which is in agreement with the observations in fMRI study [34]. This shows that children (around nine years old) do not have mature language network. Moreover, we found the difference in local correlations is more significant in the STG than the IFG, which implies the skill for language comprehension is developed later than language production.

#200752 - $15.00 USD Received 5 Nov 2013; revised 19 Jan 2014; accepted 20 Jan 2014; published 24 Jan 2014

In addition to the correlation differences in the left hemisphere, children also show weaker inter-hemispheric correlation than adults, in both the IFG and STG (see Fig. 2 and Fig. 3). A resting state fMRI study demonstrated that normal children display inter-hemispheric synchronization of cortical activity with average correlation coefficients in the IFG around 0.5 and slightly higher in the STG [25]. Our data show that children inter-hemispheric HBO correlation is 0.474 in IFG, 0.486 in STG, respectively (see Fig. 3), which is consistent with the fMRI study. The inter-hemispheric correlation values for adults in the IFG and the STG are not found in the published data, however the average correlation values in some cortical regions were measured previously by fNIRS [17], such as in prefrontal, sensorimotor and visual cortices, ranging from 0.5 to 0.7 for HBO, 0.55 to 0.8 for HB, and 0.6 to 0.75 for HBT. Our average correlation values for HBO and HBT are well within these ranges, whereas the average values for HB are around 0.45 slightly below the range.

In the adult group, the inter-hemispheric correlation map for the STG shows higher symmetry than the IFG [see Figs. 2(a) and 2(b)]. This reveals the spontaneous network activity in STG regions between the left and right is more synchronized than in the IFG. Since the STG is responsible for language comprehension, this higher resting state synchronization may imply that the brain is more efficient at processing information quickly when understanding other's words than when producing its own words.

It should be noted that correlation maps generated by choosing different seeds in the left hemisphere are visually different from each other. However, the results that children have significantly lower values for inter-hemispheric and intra-hemispheric correlations are independent of the seed choice.

The superiority of females in language ability to males is a matter of debate [26,27]. Our experimental data show there are no significant differences in correlation maps (not shown in this paper) between males and females in either the IFG or the STG areas. The average inter-hemispheric correlation coefficients for the three hemodynamic components in all areas of interest are slightly higher for females than males (see Fig. 4). However, the differences in correlation values are not statistically significant, except for HBT in STG area is marginally significant. These findings do not provide strong evidence to support differences between males and females in language ability.

5. Conclusions

fNIRS was used to record spontaneous hemodynamic fluctuations from the important language areas of the IFG and the STG. The generated correlation maps for the three hemodynamic components across two hemispheres showed clearly differences between adults and children, for both intra-hemispheric and inter-hemispheric correlations. These differences may reflect the developmental differences between adults and children in language production and comprehension. In adults, no significant sex differences on the correlations were observed, which implies that language area functioning is not distinguishable between males and females, in line with most of previous studies. Our results demonstrated fNIRS is able to identify and quantitatively evaluate the language network, which may have potential applications for diagnosing brain diseases associated with nuerodegeneration and developmental defects, such as Alzheimer's disease and autism.

Acknowledgments

This work was supported by Guangdong (China) Innovative Research Team Program (No. 201001D0104799318). We would like to thank J. Evans for language editing and useful discussions.

#200752 - $15.00 USD Received 5 Nov 2013; revised 19 Jan 2014; accepted 20 Jan 2014; published 24 Jan 2014